DOI: 10.1002/adsc.201200213

Structural and Catalytic Characterization of *Pichia stipitis* OYE 2.6, a Useful Biocatalyst for Asymmetric Alkene Reductions

Yuri A. Pompeu,[a,b] Bradford Sullivan,[a,b] Adam Z. Walton,[a,b] and Jon D. Stewart[a,*]

[a] 126 Sisler Hall, Department of Chemistry, University of Florida, Gainesville, FL 32611, USA
Fax: (+1)-352-846-0743; phone: (+1)-352-846-0743; e-mail: jds2@chem.ufl.edu
[b] These authors contributed equally to this work

Received: March 14, 2012; Revised: May 17, 2012; Published online: ■■ ■■, 0000

Supporting information for this article is available on the WWW under http://dx.doi.org/10.1002/adsc.201200213.

Abstract: We have probed *Pichia stipitis* CBS 6054 Old Yellow Enzyme 2.6 (OYE 2.6) by several strategies including X-ray crystallography, ligand binding and catalytic assays using the wild-type as well as libraries of site-saturation mutants. The alkene reductase crystallized in space group $P6_322$ with unit cell dimensions of 127.1×123.4 Å and its structure was solved to 1.5 Å resolution by molecular replacement. The protein environment surrounding the flavin mononucleotide (FMN) cofactor was very similar to those of other OYE superfamily members; however, differences in the putative substrate binding site were also observed. Substrate analog complexes were analyzed by both UV-Vis titration and X-ray crystallography to provide information on possible substrate binding interactions. In addition, four active site residues were targeted for site saturation mutagenesis (Thr 35, Ile 113, His 188, His 191) and each library was tested against three representative Baylis–Hillman adducts. Thr 35 could be replaced by Ser with no change in activity; other amino acids (Ala, Cys, Leu, Met, Gln and Val) resulted in diminished catalytic efficiency. The Ile 113 replacement library yielded a range of catalytic activities, but had very little impact on stereoselectivity. Finally, the two His residues (188 and 191) were essentially intolerant of substitutions with the exception of the His 191 Asn mutant, which did show significant catalytic ability. Structural comparisons between OYE 2.6 and *Saccharomyces pastorianus* OYE1 suggest that the key interactions between the substrate hydroxymethyl groups and the side-chain of Thr 35 and/or Tyr 78 play an important role in making OYE 2.6 an (*S*)-selective alkene reductase.

Keywords: alkenes; biocatalysis; enzyme catalysis; reduction; structural biology; X-ray diffraction

Introduction

Alkene reductase enzymes have recently emerged as powerful catalysts for asymmetric C=C reductions (for recent reviews, see ref.[1]). Pioneering work on *Saccharomyces pastorianus*[2] Old Yellow Enzyme 1 (OYE1) by Massey established that this flavoprotein reduced a variety of electron-deficient alkenes and also catalyzed a mechanistically related dismutation reaction in the absence of the physiological reductant NADPH.[3] Since then, several groups have explored synthetic applications of *S. pastorianus* OYE1 (for recent examples, see ref.[4] and references cited therein). While a number of successes have been reported, a single biocatalyst can only provide one product enantiomer.[5] We have explored two potential strategies for overcoming this limitation: accumulating a collection of native alkene reductases and applying protein engineering strategies to existing enzymes.

An ever-increasing number of putative old yellow enzyme superfamily members is available from genome sequencing projects. We and others have cloned, overexpressed and characterized these proteins with respect to their substrate and stereoselectivities in the hopes of identifying pairs of enantiocomplementary biocatalysts (summarized in ref.[6]). In the early stages, target genes were chosen on the basis of DNA availability and similarity to *S. pastorianus* OYE1. While some stereochemical diversity was observed, the vast majority of old yellow enzyme homologs had essentially the same catalytic properties. Some of our earliest protein engineering studies revealed that replacing an active site Trp residue (position 116) with Ile radically changed the stereoselectivity of *S. pastorianus* OYE1,[7] an observation later

Table 1. OYE 2.6 data collection and refinement statistics.

Accession code	3TJL	3UPW	4DF2
Observed active site ligand	malonate	nicotinamide/malonate	*p*-chlorophenol
X-ray source	NSLS X25	NSLS X25	Rigaku CuKα
Space group	$P6_322$	$P6_322$	$P6_322$
Unit cell dimensions			
$a=b$, c (Å)	127.16, 122.45	127.30, 123.06	127.73, 123.64
Resolution (Å)	44.10–1.50	44.24–1.78	24.86–2.02
Unique reflections	92,358 (2,365)[a]	56,484 (1,608)	38,149 (1,269)
Completeness (%)	99.07 (96.0)	99.76 (96.0)	96.70 (99.0)
Redundancy	7.6 (4.7)	10.5 (4.2)	7.2 (6.9)
R_{merge}[b]	0.056 (0.60)	0.047 (0.55)	0.093 (0.70)
I/σ (I)	33.4 (2.0)	37.1 (2.1)	14.2 (2.1)
R_{work}[c], R_{free}[d]	0.143, 0.168	0.157, 0.185	0.160, 0.198
Ramachandran statistics[e]			
Favored (%)	97.60	97.80	97.52
Allowed (%)	2.40	2.20	2.48
Outliers (%)	0	0	0
Number of protein, solvent and ligand atoms	3,238, 517, 52	3,211, 445, 65	3,218, 394, 53
Average B factors (Å^2)			
Protein	22.21	23.20	31.40
Solvent	35.20	34.40	38.87
FMN	16.22	19.17	26.21
Ligands	33.30, 28.40, 23.10	34.90, 31.80, 38.0 (malonate); 21.70 (nicotinamide)	39.30, 26.20 (malonate); 27.01 (*p*-chlorophenol)

[a] Values in parentheses denote data for the highest resolution bin (1.53–1.50 Å, 1.81–1.78 Å, 2.09–2.02 Å).
[b] $R_{merge}=\Sigma\,|I-<I>|/\Sigma<I>$.
[c] $R_{work}=\Sigma|F_o(hkl)|-|F_c(hkl)|/\Sigma|F_o(hkl)|$.
[d] R_{free} is calculated in the same manner as R_{work} using 10% of the reflection data not included during the refinement.
[e] Statistics generated using MOLPROBITY.[18]

confirmed by a more systematic investigation.[4a] We therefore sought old yellow enzyme homologs possessing residues other than Trp at the position corresponding to 116 of *S. pastorianus* OYE1. This prompted us to clone and overexpress the OYE 2.6 gene from the xylose-fermenting yeast *Pichia stipitis* CBS 6054.[8] Based on sequence alignment and computer modeling from the *S. pastorianus* OYE1 structure, Ile 113 in OYE 2.6 was expected to occupy a similar active site location as Trp 116. On this basis, we expected that the stereoselectivity of OYE 2.6 would be analogous to that of the *S. pastorianus* OYE1 Trp 116 Ile mutant; however, the reality proved more complex.

In general, OYE 2.6 has proven to be a superior alkene reductase with regard to stereoselectivity, conversion rate and stability.[9] In some cases, its stereoselectivity was opposite that of *S. pastorianus* OYE1, but this was not universally true. There are currently two impediments to the wider use of OYE 2.6 in chemical synthesis: a relatively limited knowledge of substrate and stereoselectivity characteristics and an unknown three-dimensional structure. Because the latter is particularly critical for protein engineering studies of this enzyme, solving the X-ray crystal structure of OYE 2.6 has been a priority and the results are reported here. In addition, we also provide the results of four site-saturation mutagenesis libraries that allow for meaningful comparisons with *S. pastorianus* OYE1 and also point the way toward future approaches to obtaining even more useful variants of OYE 2.6.

Results and Discussion

Native OYE 2.6 was overexpressed in *E. coli* and purified by ammonium sulfate fractionation followed by affinity[10] and gel filtration chromatography. After screening approximately 300 conditions, crystals were observed when organic salts were the main precipitants at near-neutral pH values. The most promising, obtained in 2.4 M sodium malonate, pH 7.0, diffracted to a maximum resolution of 2.0 Å using a Rigaku Cu rotating anode X-ray source. Unfortunately, these proved unsuitable for crystallographic studies as they

were not singular and yielded diffraction patterns that could not be indexed accurately. Because attempts at optimizing pH and salt concentrations proved unsuccessful, a further screening of 96 additives coupled with the original conditions (2.4 M sodium malonate, pH 7.0) was carried out. Buffer containing 1–3% 2-propanol yielded crystals that diffracted to a maximum usable resolution of 1.5 Å using synchrotron source radiation. The unit cell measured 127.1 × 123.4 Å and the crystals belonged to space group $P6_322$. The asymmetric unit contained one molecule and a solvent content of 63% with a Matthews coefficient of 3.23 $Å^3$/Dal.[11]

The initial OYE 2.6 structure (with no added ligand) was solved by molecular replacement[12] using *S. pastorianus* OYE1 as the search model (1OYA).[13] The final OYE 2.6 model was refined to 1.5 Å resolution with final values of R_{work} and R_{free} of 0.143 and 0.168, respectively (Table 1). The enzyme exhibits the eight-stranded α/β-barrel fold first seen in triosephosphate isomerase (TIM) and glycolate oxidase (GOX) and belongs to the TIM phosphate binding family (Figure 1, **A**).[14] The overall structure of OYE 2.6 is similar to those of other old yellow enzyme homologs, particularly OYE1 from *S. pastorianus*. These share 43% sequence identity and also have closely related backbone positioning (aligning 325 α-carbons yielded a root mean square deviation of 0.92 Å; Figure 1, **B**). The next most similar structures are *Pseudomonas putida* morphinone reductase (MR, 1GWJ)[15] (291 *Cα* aligned, 1.26 Å r.m.s.d.), *Enterobacter cloacae* pentaerythritol tetranitrate reductase (PETNR, 1H50)[16] (232 *Cα* aligned, 1.38 Å r.m.s.d.), followed by *Bacillus subtilis* YqjM (1Z41)[17] (191 *Cα* aligned, 2.57 Å r.m.s.d.). The most important structural difference between *P. stipitis* OYE 2.6 and *S. pastorianus* OYE1 is found in loop L6 (Glu 287–Ala 302) (Figure 1, **B**). Most of the key active site residues are conserved between OYE 2.6 and OYE1, suggesting that these can be grouped into the same class of OYE homologs. *S. pastorianus* OYE1 is dimeric, both in solution[19] and in the crystal state.[13] Gel filtration chromatography indicated that *P. stipitis* OYE 2.6 is also a dimer in solution (data not shown), and an analysis of subunit-subunit contacts is also consistent with a dimer that buries a total of 1520 $Å^2$ at the interface region. This was further corroborated by PISA analysis,[20] which predicted that OYE 2.6 would form a stable homodimer with a predicted $\Delta G_{diss} = 5.0$ kcal/mole). Interestingly, despite crystallizing in a different space group ($P6_322$ for OYE 2.6 *versus* $P4_32_12$ for *S. pastorianus* OYE1), the relative positions of the two monomers are nearly identical and, in both cases, the monomers are related by a 2-fold crystallographic symmetry operator.

The constellation of amino acid side chains that interact with FMN in OYE 2.6 is highly conserved in other OYE family members. The well-defined and well-ordered cofactor (all B-factors ≈ 10 $Å^2$) is bound in the center of the enzyme's parallel 8 strand β-barrel (see Supporting Information). Its negatively charged phosphate group interacts directly with Arg 347, a highly conserved residue among members of the family. Oxygen *O3′* appears to hydrogen bond with both water 31 and Arg 240, whose side chain also interacts indirectly with *O2′*. The dimethylbenzene moiety of FMN makes contacts with the aromatic residues Phe 373 and Tyr 374 and its isoalloxazine ring is positioned to form direct hydrogen bonds with

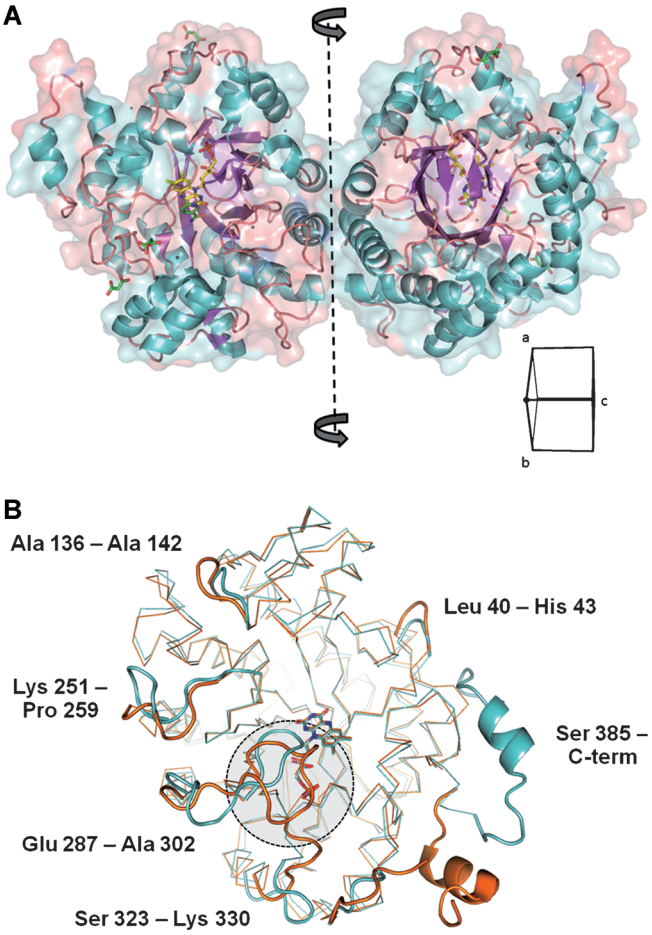

Figure 1. Structure of *P. stipitis* OYE 2.6. **A**: Overall structure of the OYE 2.6 homodimer. The dashed line indicates the molecular two-fold axis, which is parallel to the crystallographic a,b plane. The enzyme exhibits a TIM barrel fold and the backbone is colored by secondary structure motifs (α-helices, cyan; β-sheets, magenta; loops, pink). Bound ligands (FMN and nicotinamide) are shown as sticks. The solvent-accessible surface is shown for reference. **B**: Aligned structures of *P. stipitis* OYE 2.6 (cyan) and *S. pastorianus* OYE1 (orange). Enzyme backbones are depicted in ribbon representation with regions of highest deviation shown as cartoons for clarity. Numbers refer to the OYE 2.6 amino acid sequence. Loop 6 lies above the ribityl chain of the FMN cofactor and is outlined by a dashed circle.

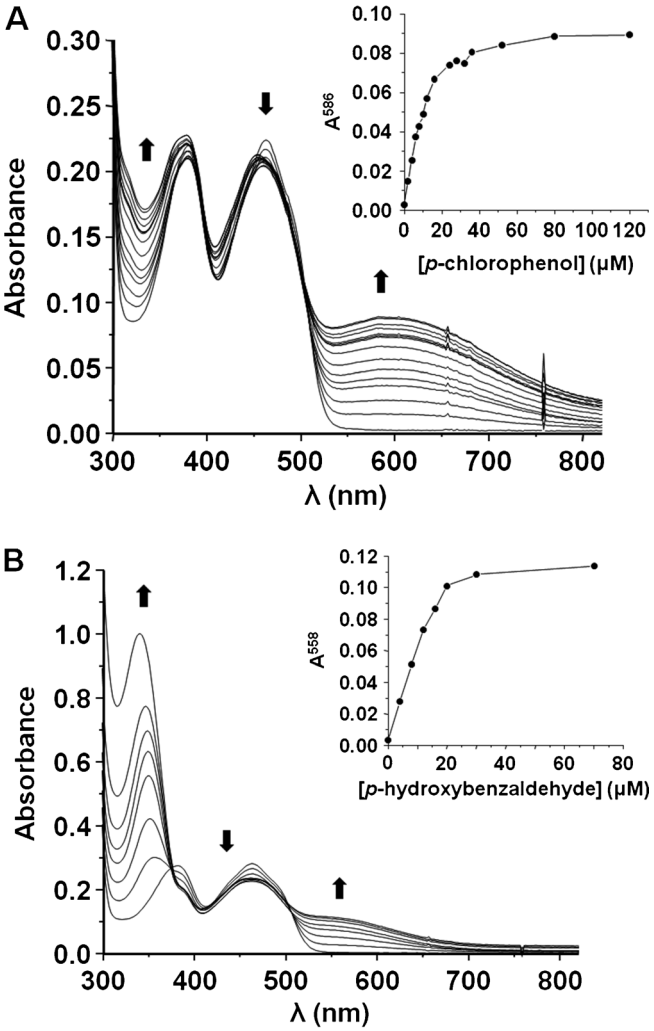

Figure 2. Phenol binding to OYE 2.6. **A**: *p*-Chlorophenol; aliquots of *p*-chlorophenol were added to a 21.0 μM solution of OYE 2.6 to give final ligand concentrations of 2, 4, 6, 8, 10, 12, 16, 24, 28, 32, 36, 52, 80 and 120 μM. UV-Vis spectra were recorded after each addition. *Inset*: A^{586} *versus* [*p*-chlorophenol]. **B**: *p*-Hydroxybenzaldehyde; aliquots of *p*-hydroxybenzaldehyde were added to a 26.6 μM solution of OYE 2.6 to give final ligand concentrations of 4, 8, 12, 16, 20, 30 and 70 μM. UV-Vis spectra were recorded after each addition. *Inset:* A^{558} *versus* [*p*-hydroxybenzaldehyde].

Gln 111, Thr 35, Arg 240 and the main chain nitrogen of Ala 68. Gln 111 is highly conserved in the OYE family and this side chain, along with that of Thr 35, is implicated in regulating the FMN reactivity in *S. pastorianus* OYE1.[21]

We used spectral changes that accompany phenol binding to OYE 2.6 to characterize its active site character and cofactor properties (Figure 2).[22] OYE 2.6 bound both *p*-chlorophenol and *p*-hydroxybenzaldehyde tightly and these complexes were accompanied by long wavelength charge transfer bands with λ_{max} at *ca.* 586 and 558 nm, respectively. Massey determined that the positions of these charge transfer bands for *S. pastorianus* OYE1 depended upon both hydrogen bonding interactions with the phenol(ate) oxygen and the FMN reduction potential.[22c] In OYE1, the phenolic oxygen lies near the side chains of His 191 and Asn 194; by contrast, two histidines occupy these positions in OYE 2.6 (His 188 and 191). Compared with the corresponding values for *S. pastorianus* OYE1, λ_{max} values for both *p*-chlorophenol and *p*-hydroxybenzaldehyde interacting with OYE 2.6 are blue-shifted by 59 and 27 nm, respectively. Relatively small effects on charge-transfer λ_{max} values were observed from changing phenol(ate) hydrogen bonding partners in OYE1,[23] whereas substituting the enzyme with FMN analogs possessing different reduction potentials led to more significant wavelength shifts.[24] Given the similarity in active site structures between OYE 2.6 and OYE1, the differences in charge-transfer λ_{max} values are therefore more likely to reflect small differences in flavin electronic properties. Using the relationships between FMN $E^{\circ\prime}$ and λ_{max} values for *p*-chlorophenol and *p*-hydroxybenzaldehyde established for *S. pastorianus* OYE1,[22c] we estimated that the $E^{\circ\prime}$ value for OYE 2.6 is *ca.* −215 mV. This is similar to that measured for wild-type OYE1 (−230 mV).[24]

The initial OYE 2.6 crystals displayed electron density above the *si* face of the FMN that could be well fit by malonate, which was present in the crystallization buffer (Figure 3, **A**). In this complex, one carboxylate oxygen was positioned to form hydrogen bonds with the side chains of histidines 188 and 191, which likely mimics their interactions with the carbonyl oxygens of conjugated alkene substrates (*vide infra*). The other carboxylate oxygen formed a hydrogen bond with an ordered water molecule (WAT 301) that also interacted with the side-chains of Tyr 78 and Thr 35. While several well-ordered malonate molecules were observed in the crystal, only this active site malonate was found in the higher energy planar conformation (all solvent-exposed malonates were observed in the expected bent form).

Crystals grown from a second preparation of OYE 2.6 also showed additional electron density in the active site region; however, the shape differed significantly from that observed previously and was consistent with free nicotinamide at an occupancy of *ca.* 95% (Figure 3, **B** and Table 1).[25] This fortuitous complex likely mirrors that between OYE 2.6 and its natural substrate, NADP(H). The amide carbonyl oxygen is located within hydrogen bond distances of the imidazole side chains of both His 188 and His 191 and the distance and angle between the nicotinamide *C*4 and the FMN are consistent with the geometry of hydride transfer (3.4 Å and 94°, respectively).[26] Further supporting the notion that this arrangement mimics the productive NADPH/OYE 2.6 Michaelis complex, the nicotinamide binding orientation within OYE 2.6 is analogous to those observed for tetrahy-

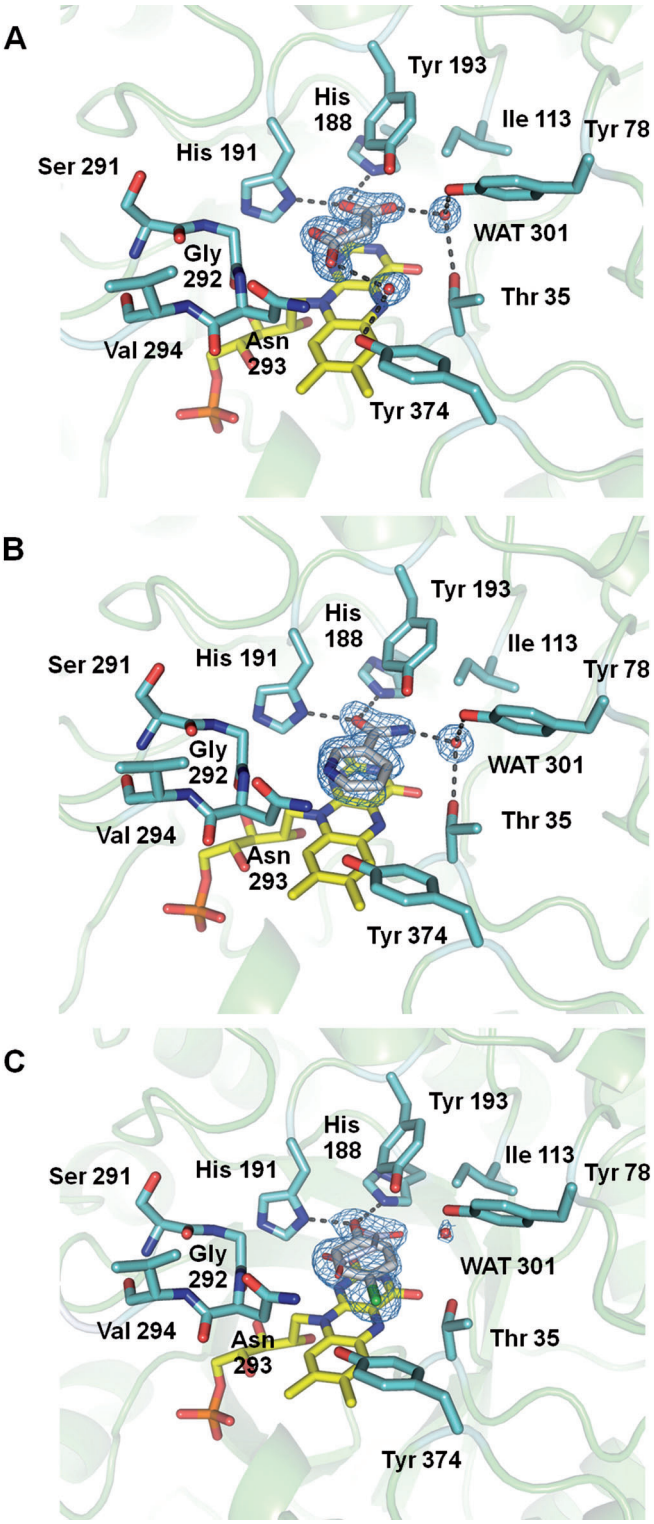

Figure 3. Ligand interactions with the active site of OYE 2.6. **A**: Malonate complex; the simulated annealing composite omit map contoured at the 1.5 σ level is shown for bound malonate and two ordered water molecules. Potential hydrogen bonds with the side chains of histidines 188 and 191 are shown by dashed lines. **B**: Nicotinamide complex; the simulated annealing composite omit map contoured at the 1.2 σ level is shown for the ligand and an ordered solvent molecule. Potential hydrogen bonds are indicated by dashed lines. **C**: *p*-Chlorophenol complex; the simulated annealing composite omit map contoured at the 0.5 σ level is shown for the ligands and an ordered water molecule. Partial occupation by malonate and *p*-chlorophenol was observed and modeled. Potential hydrogen bonds are indicated by dashed lines.

dronicotinamide within the active sites of *Thermoanaerobacter pseudethanolicus* TOYE[27] and morphinone reductase.[28] Unfortunately, neither UV-Vis nor fluorescence spectroscopy yielded usable spectral changes for nicotinamide binding to OYE 2.6, so its binding constant could not be measured by these methods.

To provide a model for how potential substrates might bind to the active site of OYE 2.6, the *p*-chlorophenol complex was prepared by soaking crystalline OYE 2.6 in cryoprotectant buffer containing 2 mM inhibitor (Figure 3, **C**). The phenolic oxygen was positioned between the side chains of His 188 and 191 and a *meta* ring carbon was 3.5 Å above the FMN N5 atom. The angle between this carbon and N5 and N10 of the FMN was 105°. These values are consistent with those expected for efficient hydride transfer to a cyclohexenone β-carbon.

After structural characterization of OYE 2.6 was completed, we turned our attention to probing its structure/function relationships with respect to alkene reductions. We chose three representative Baylis–Hillman adducts **1**–**3** for catalytic studies of OYE 2.6 (Figure 4) since they possess additional functionality that makes them suitable for further useful chemical transformations following asymmetric alkene reductions.[29] While a number of catalytic hydrogenation strategies for the asymmetric reduction of **3** has been reported (for recent examples, see ref.[30] and references cited therein), we are not aware of similar catalysts being applied to cyclic enones **1** and **2**. In addition, we have previously used the same series for characterizing *S. pastorianus* OYE1 mutants, thereby facilitating direct comparison of their substrate and stereoselectivities.[4a]

We created four site-saturated mutagenesis libraries of OYE 2.6 using a variation of the Reymond method and a reduced genetic alphabet (NNK) that contained 32 codons but still encompassed all twenty amino

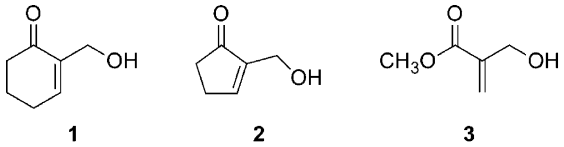

1 2 3

Figure 4. Baylis–Hillman adducts tested as substrates.

acids.[31] After extensive optimization, libraries routinely contained $\geq$16 amino acid replacements (usually 18 or 19). After verifying their diversity at the pooled plasmid DNA stage, this mixture was used to transform the *E. coli* expression host, individual clones were seeded in 95 wells (the last contained wild-type control) and all plasmids present in the plate were sequenced. For every randomized amino acid position, a representative of each codon (when available) was arrayed on one third of a 96 well plate to eliminate redundant screening efforts. In the case of the Ile 113 library, simple site-directed mutagenesis methods were used to obtain the three missing codons so that a complete set of amino acid replacements could be screened.

Enones **1**–**3** were reduced under whole-cell conditions in the presence of glucose for NADPH regeneration by host metabolic pathways. OYE 2.6 was overexpressed as a fusion protein with glutathione *S*-transferase. Reaction conditions (cell mass and reaction time) were chosen so that the wild-type enzyme afforded *ca.* 99% conversion for substrates **1** and **2** and 75% conversion for substrate **3** during the biotransformations. Reaction progress and product enantiopurities were assessed by chiral-phase GC. Controls reactions verified that racemization did not occur during the biotransformations (data not shown).

Histidine 188 in OYE 2.6 showed little tolerance toward amino acid substitutions and only the wild-type protein was highly active (see Supporting Information). The Ser, Gln and Asn variants reduced **1** and **2** poorly but showed no detectable activity toward **3**. All variants retaining catalytic activity showed the same (*S*)-stereoselectivity as the wild-type enzyme. In *S. pastorianus* OYE1, the corresponding position (191) is also occupied by His. This residue was changed to Asn by Massey; while the variant retained catalytic activity, the K_M value for 2-cyclohexenone increased significantly.[23] The differential response toward analogous substitutions highlights the subtle differences in active site architecture, even among highly similar alkene reductases. Despite the lack of success in identifying functional histidine replacements in this particular case, others have found that site-saturation libraries can sometimes reveal unexpected results.[32] Scrutton mutated the corresponding His residue in *E. cloacae* PETNR (position 181) and found that this library had very low average catalytic activity when tested against carbonyl-conjugated alkenes.[33] On the other hand, several useful replacements for *E. cloacae* PETNR His 181 were identified for nitroalkenes.[34]

Position 191 in OYE 2.6 was slightly more tolerant toward mutation, with both the native His and the Asn mutant proteins showing significant catalytic activity (see Supporting Information). No changes in enantioselectivity were observed for the three enones investigated here. As observed in the previous case, the catalytic activities of the mutant proteins were generally consistent across all three enone substrates. This underscores the point that the catalytic assays reveal general characteristics of the enzymes and suggests that similar behavior will apply to other potential substrates as well. The analogous position in *S. pastorianus* OYE1 (194) contains Asn. Interestingly, attempts to prepare the single Asn 194 His mutant of *S. pastorianus* OYE1 were unsuccessful.[23] The analogous His in *E. cloacae* PETNR (position 184) also showed limited tolerance for amino acid replacement, although the Asn mutant retained 20% of the wild-type activity for 2-cyclohexenone.[33,34] Several PETNR library members showed improved stereoselectivity for nitroalkenes.[35]

In both OYE 2.6 and *S. pastorianus* OYE1, the side-chain of a key Thr residue forms a hydrogen bond with O4 of the bound FMN. For OYE1, loss of this interaction (in the Thr 37 Ala mutant) slowed the reductive half-reaction by an order of magnitude but increased the oxidative half-reaction.[21a] Other OYE family members contain Thr or Cys at the analogous position. Based on these precedents, we created and examined a systematic replacement library for Thr 35 in OYE 2.6 (Figure 5, **A**). For OYE 2.6, the Ser replacement had essentially the same properties as the wild-type enzyme, consistent with the importance of hydrogen bonding with the FMN cofactor. The Ala variant also possessed activity, albeit diminished. The most surprising result was that several other residues (Cys, Leu, Met, Gln and Val) could also functionally replace Thr 35, though with lower efficiencies. No change in stereoselectivity was found for any of the Thr 35 substitutions. The observed tolerance toward changes at this position bodes well for future work in active site remodeling.

Substitutions at the analogous position of other OYE family members have also been reported. Like OYE 2.6, this position is occupied by Thr in wild-type *E. cloacae* PETNR (position 26). A site-saturation library of replacements gave very low average activity; however, both Ala and Ser substitutions were functional.[33] As part of a larger iterative saturation mutagenesis study of *B. subtilis* YqjM, Bougioukou et al. examined substitutions for Cys 26 (corresponding to Thr 35 in OYE 2.6).[36] For one model enone substrate, YqjM tolerated a number of substitutions at this position, although the impacts on conversion and stereoselectivity were modest. Interestingly, the effect of these substitutions was increased significantly by additional changes elsewhere in the active site, supporting the notion that this position in OYEs plays an important cooperative role in governing their properties.

Our previous studies of *S. pastorianus* OYE1 highlighted the key influence of Trp 116 in controlling re-

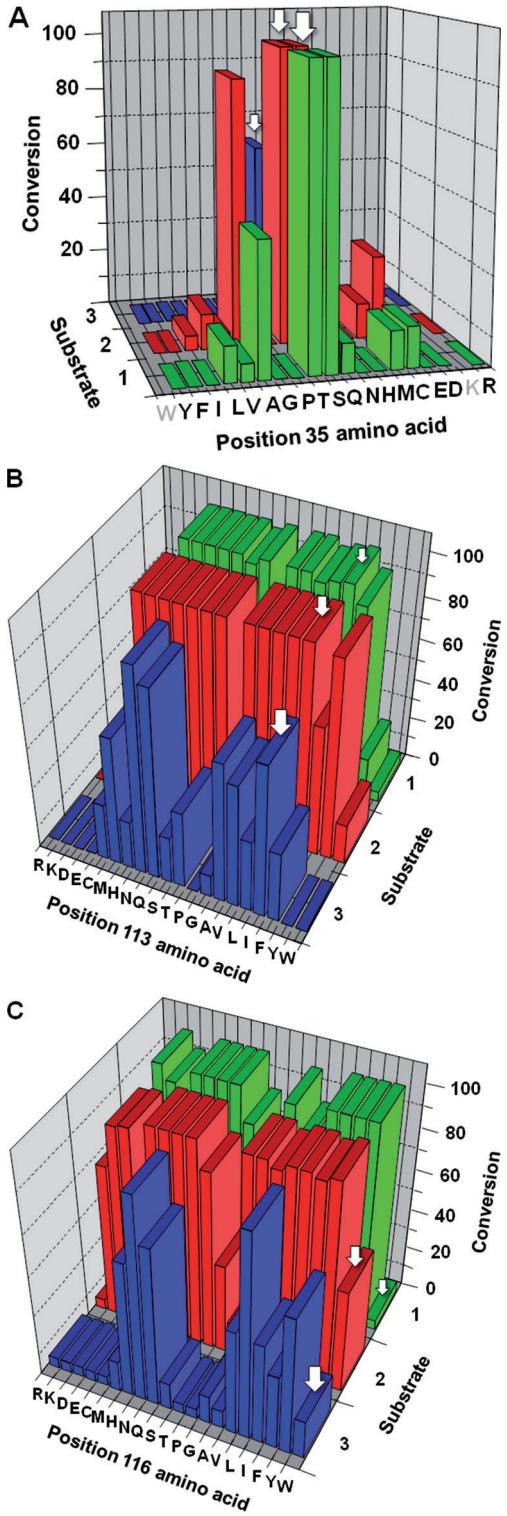

Figure 5. Site-saturation mutagenesis results for key active site residues. **A**: Thr 35 of OYE 2.6. OYE 2.6 variants with all possible replacements for Thr 35 (except Trp and Lys) were screened for reductions of Baylis–Hillman adducts **1**, **2** and **3** using whole-cell assays. Arrows indicate data for the wild-type enzyme and amino acids shown in grey were absent from the library. **B**: Ile 113 of OYE 2.6; variants with all possible replacements for Ile 113 were screened for reductions of Baylis–Hillman adducts **1**, **2** and **3** using whole-cell assays. Arrows indicate data for the wild-type enzyme. **C**: Trp 116 of *S. pastorianus* OYE1; variants with all possible replacements for Trp 116 were screened for reductions of Baylis–Hillman adducts **1**, **2** and **3** using whole-cell assays. Arrows indicate data for the wild-type enzyme.

activity[4a,7] and similar observations have been made for both *E. cloacae* PETNR[33] and *B. subtilis* YqjM.[36] As noted above, the corresponding position in native OYE 2.6 (113) is occupied by Ile. A number of amino acids was tolerated by OYE 2.6 at position 113 (Figure 5, **B**). Small-to-medium hydrophobic residues (Ala, Leu, Met, Phe and Val) as well as polar, uncharged amino acids (Asn, Cys, Gln, His, Ser and Thr) could replace the native Ile with good to excellent retention of catalytic activity. On the other hand, charged amino acids, Pro and larger hydrophobic residues (Tyr and Trp) yielded inactive proteins toward the Baylis–Hillman adducts examined here. One difference between the position 113 mutants and the libraries described above is that conversions differ significantly between the two cyclic enones and the acyclic Roche ester precursor.

With regard to substrate conversion, the response of OYE 2.6 toward amino acid substitutions at position 113 closely mirrors that of a Trp 116 replacement library in *S. pastorianus* OYE1 (Figure 5, **C**).[4a] Like OYE 2.6, OYE1 prefers cyclic enones **1** and **2** over acyclic alkene **3** and similar ranges of residues at position 116 are acceptable substitutes for the native Trp. In some cases, this similarity extends to changes in stereoselectivity. For example, wild-type OYE1 (with Trp at position 116) reduces **2** with predominantly (*R*)-selectivity (60% *ee*); by contrast, the Trp 116 Ile mutant afforded 91% *ee* (*S*)-product.[4a] For OYE 2.6, wild-type (with Ile at position 113) reduced **2** with high (*S*)-selectivity (>90% *ee*) while the Ile 113 Trp mutant provided 11% *ee* favoring the (*R*)-enantiomer.

One important difference between the behavior of OYE 2.6 and *S. pastorianus* OYE1 mutants involves Roche ester precursor **3**. Wild-type OYE 2.6 and all of the Ile 113 mutants that accept this substrate catalyze reductions with essentially complete (*S*)-selectivity, although some with relatively poor conversion. By contrast, mutating Trp 116 in *S. pastorianus* OYE1 provides a range of stereoselectivities for this substrate, ranging from >98% *ee* (*R*) (wild-type) to >98% *ee* (*S*) (Trp 116 Gln).[4a] These differences highlight the distributive nature of the substrate binding pocket within alkene reductases. While single amino substitutions can be sufficient to alter stereoselectivity in some favorable cases, multiple substitutions are more often required. Comparing the structures of OYE 2.6 and *S. pastorianus* OYE1 in light of these

mutagenesis data provides a much better roadmap for future protein engineering studies.

Conclusions

A major motivation for determining the crystal structure of OYE 2.6 was to understand its stereoselectivity, particularly why it is generally opposite to that of wild-type *S. pastorianus* OYE1 for Baylis–Hillman adducts **1**–**3** (but identical to that of the OYE1 W116I mutant). In two of our three OYE 2.6 structures, an ordered water molecule hydrogen bonds to the side-chains of Thr 35 and Tyr 78 (Figure 3, **A** and **B**). When the FMN moieties of the OYE 2.6/malonate complex and the *S. pastorianus* W116I OYE1/enone **2** complex were overlaid, the hydroxy group of **2** was in the same location as these ordered water molecules in OYE 2.6 (Figure 6). Our previous results have argued that this protein-substrate interaction in *S. pastorianus* OYE1 plays a key role in determining which face of the alkene π system will accept hydride from reduced FMN.[4a] It is therefore reasonable to suggest that an analogous hydrogen bond is also formed between OYE 2.6 and the hydroxymethyl groups of **1**–**3** and this provides a structural rationale for the observed stereoselectivity. We carried out structural alignments of OYE 2.6 with wild-type[13] and the W116I mutant[4a] *S. pastorianus* OYE1, morphinone reductase (MR),[15] pentaerythritol tetranitrate reductase (PETNR),[16] YqjM,[17] *Thermoanaerobacter pseudethanolicus* E39 TOYE (3 KRZ)[27] and tomato oxophytodienoate reductase OPR1 (1ICS)[37] to determine whether these proteins also contain an analogous ordered water molecule. Interestingly, this water was only observed near the FMN in OYE 2.6. In the case of OYE1, MR, PETNR and OPR1, a tryptophan residue fills this volume and eliminates the possibility of an ordered water molecule at this location. Both YqjM and TOYE possess Ala in this location that provides sufficient space; however, the two residues that form hydrogen bonds with the ordered water in OYE 2.6 (Thr 35 and Tyr 78) either cannot form hydrogen bonds (Ile) or have a suitable residue (Cys), but in unfavorable orientations. Taken together, this may explain the absence of this critical ordered water molecule in the other proteins.

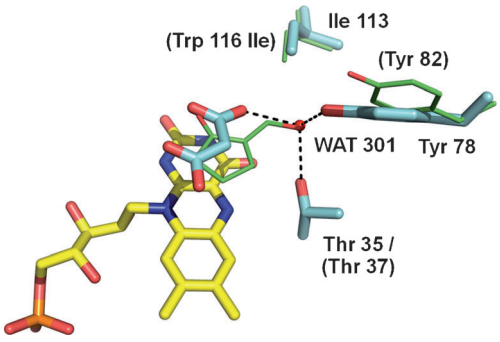

Figure 6. Comparison of OYE 2.6 and *S. pastorianus* OYE1 complexes. The structures of native OYE 2.6 with bound malonate (cyan, 3TJL) and the structure of the *S. pastorianus* W116I OYE1 mutant with enone **2** present in the productive binding orientation (green, 3RND) were overlaid using all FMN atoms (yellow carbons). Key side-chains and an ordered water molecule are shown (OYE 2.6 numbering is shown with the corresponding residues for *S. pastorianus* OYE1 in parentheses). For clarity, only the OYE 2.6 atoms are shown for the side-chain of Thr 35 and the FMN cofactor since the corresponding atoms of *S. pastorianus* OYE1 are found in identical positions.

The positions of the active site Thr side-chains (positions 35 and 37 in OYE 2.6 and *S. pastorianus* OYE1, respectively) are essentially indistinguishable. The same is true for the Ile side-chain (Ile 113 in OYE 2.6 and the W116I side-chain in *S. pastorianus* OYE1), with one important difference. In the OYE1 mutant, the Ile side-chain was observed in two conformations, only one of which allows productive substrate binding. Likewise, two binding orientations of enone **2** were observed in the complex with W116I *S. pastorianus* OYE1, one potentially relevant to catalysis and the other clearly incorrect.[4a] By contrast, the corresponding Ile side-chain in OYE 2.6 (Ile 113) was only found in a single conformation, which matched the productive arrangement in the W116I *S. pastorianus* OYE1 mutant (Figure 6). This singular conformation of Ile 113 may be one reason that OYE 2.6 is a more efficient catalyst when compared to the W116I mutant of *S. pastorianus* OYE1.

Despite these similarities, there are also key differences between OYE 2.6 and *S. pastorianus* OYE1 – even the OYE1 W116I mutant. For example, when reducing (*S*)-carvone, both wild-type *S. pastorianus* OYE1 and OYE 2.6 share the same stereoselectivity, which is opposite that of the OYE1 W116I mutant.[7] This not only points out the special nature of Baylis–Hillman substrate binding to alkene reductase active sites, but also underscores the fact OYE 2.6 is not simply the same as the W116I mutant of *S. pastorianus* OYE1. Other active site residues of OYE 2.6 must also influence the orientation of substrate binding. We are currently preparing and evaluating additional OYE 2.6 mutants and their complexes with potential substrates in order to understand these factors more completely.

Experimental Section

General

Restriction endonucleases, Phusion Hot Start II High-Fidelity DNA Polymerase and T4 DNA ligase were purchased

from New England Biolabs. Primers were obtained from Integrated DNA Technologies. Authentic (*R*)-Roche ester {measured $[\alpha]_D^{22}$: −15.9 (*c* 5.59, $CHCl_3$)} was obtained from Sigma. Crystallography screening kits (Classics Suite II/$AmSO_4$ and Additives kit) and were purchased from Qiagen and Hampton Research, respectively. All other reagents were obtained from commercial suppliers and used as received. Plasmids were purified on small scales by EconoSpin columns (Epoch Life Sciences) and on large scales using CsCl density gradient ultracentrifugation.[38] DNA sequencing was carried out by the University of Florida ICBR using capillary fluorescence methods using either standard protocols (single samples) or rolling circle amplification (96 well plates). LB medium contained 5 g/L Bacto-Yeast Extract, 10 g/L Bacto-Tryptone and 10 g/L NaCl. ZYP-5052 auto-inducing media contained 10 g/L tryptone, 5 g/L yeast extract, 1 mM $MgSO_4$, 25 mM $(NH_4)_2SO_4$, 50 mM KH_2PO_4, 50 mM Na_2HPO_4, 5 g/L glycerol, 0.5 g/L anhydrous glucose and 2 g/L α-lactose monohydrate.[39]

Chiral-phase GC analyses were carried out with a 30 m × 0.25 mm β-Dex 225 column (Supelco) with He as the carrier gas and detection by FID. For analysis of substrates **1** and **2** and their reduction products, the temperature program involved 140 °C for 10 min followed by a 20 °C min^{-1} increase to 200 °C, which was maintained for 3 min. Under these conditions, the (*S*)- and (*R*)-reduction products from **1** eluted at 10.1 min and 10.6 min, respectively, and the (*R*)- and (*S*)-reduction products from **2** eluted at 10.4 and 11.4 min, respectively. Starting materials **1** and **2** eluted at 13.0 and 13.1 min, respectively. For analysis of enone **3** and its reduction products, the temperature program involved 100 °C for 12 min followed by a 20 °C min^{-1} increase to 180 °C, which was maintained for 5 min. Under these conditions, the (*S*)- and (*R*)-reduction products eluted at 10.8 and 11.4 min, respectively, and the starting material was observed at 12.1 min. Representative chromatograms of starting materials and racemic products are provided in the Supporting Information.

Expression and Purification of Native *P. stipitis* OYE 2.6

E. coli BL21 (DE3) harboring plasmid pBS3 (a derivative of pET 26b containing the OYE 2.6 coding region flanked by *Nde*I and *Xho*I sites) was grown at 37 °C in LB medium supplemented with 50 μg/mL kanamycin. IPTG was added to a final concentration of 400 μM when the culture had reached an OD_{600} value of 0.6 and shaking was continued at 30 °C for an additional 8–10 h. Cells were harvested by centrifugation at 5,000 × *g*, resuspended in 100 mM Tris-Cl, 10 μM PMSF, pH 8.0 at a concentration of 1 g/mL and lysed by a French pressure cell at 12,000 psi. All purification steps were carried out at 4 °C. Debris was removed by centrifugation (18,000 × *g* for 45–60 min). Solid ammonium sulfate was added to the supernatant to reach 78% saturation, then insoluble material was removed by centrifugation (18,000 × *g* for 30 min). The pellet was resuspended in a minimal volume of 100 mM Tris-Cl, 50 mM $(NH_4)_2SO_4$, pH 8.0, then protamine sulfate was added to a final concentration of 1 mg/mL and the resulting insoluble material was removed by centrifugation (15,000 × *g* for 20 min). The dark yellow supernatant was dialyzed against 100 mM Tris-Cl, 50 mM $(NH_4)_2SO_4$, pH 8.0 for 8 h. This was replaced by additional dialysis buffer supplemented with 10 mM sodium dithionite for 6 h. In the final dialysis step (8 h), sodium dithionite was omitted from the buffer, yielding a bright yellow dialysate. The crude protein sample was loaded onto an *N*-(4-hydroxybenzoyl)aminohexyl agarose affinity column[10] previously equilibrated with 100 mM Tris-Cl, 50 mM $(NH_4)_2SO_4$, pH 8.0. The column matrix became dark brown, indicating successful OYE 2.6 binding. After loading, the column was washed with the starting buffer at a flow rate of 0.5 mL min^{-1} until the A_{280} value of the eluant stabilized at *ca.* 0.2. OYE 2.6 was eluted by washing the column with deoxygenated starting buffer supplemented with 4 mM sodium dithionite. The protein fractions with the most intense yellow color (after subsequent air oxidation) were pooled and concentrated by ultrafiltration to approximately 10 mg mL^{-1}. Final purification was achieved by gel filtration chromatography on a Superdex 200 column (Pharmacia) equilibrated with 30 mM Tris-Cl, 30 mM NaCl pH 7.5. The eluted protein was concentrated by ultrafiltration to *ca.* 40 mg mL^{-1} (using a calculated ε^{280} value of 55,810)[40] prior to crystallization studies.

Crystallogenesis

Crystals were grown using the sitting drop vapor diffusion method from 2.4 M sodium malonate, pH 7.0 buffer supplemented with 1–3% 2-propanol. After growth, crystals were soaked in harvesting buffer (3.0 M sodium malonate, 10% v/v glycerol, pH 7.0) and flash frozen in liquid nitrogen for data collection. The crystals belonged to space group $P6_322$. To prepare the *p*-chlorophenol complex, crystals were briefly soaked in harvesting buffer supplemented with 2 mM *p*-chlorophenol. Increasing soaking times increased mosaicity and decreased the resolution of the crystals. The best results (diffraction to 2.02 Å) resulted from soaking for 5 seconds.

Structure Solution

Reflection data were processed using the HKL3000 program suite.[41] Phases were obtained by molecular replacement using the AutoMR utility of PHENIX.[12] using a modification of *S. pastorianus* OYE1 (PDB code 1OYA) as the search model. All ligands, water molecules and non-identical side-chains were removed prior to molecular replacement. One solution was found in space group $P6_322$. Moreover, the initially calculated $2F_o$-F_c and F_o-F_c maps showed electron density patterns that could be easily identified as FMN, further validating the molecular replacement solution. The initial model consisted of 385 amino acids (most devoid of side chains) and an R_{free} value of 0.33. After the initial simulated annealing refinement followed by refinement with individual xyz parameters and B-factors, the R_{free} dropped to 0.24. Inspection of the newly-phased electron density maps allowed placement of the missing residues and showed that some regions of the protein backbone required rebuilding. Refining the more complete model improved the phases and electron density maps clearly showed both ordered solvent molecules and amino acid side chains. Iterative cycles of model-building and refinement were continued to yield the final protein structures. Model building was carried out with COOT[42] and refinement was performed by PHENIX. After the protein and cofactor modeling was completed, additional electron density lying above the FMN was apparent

Table 2. Primers used for library creation.

Position	Sequences
35 Forward	5′-ATCCACCAACT**NNK**AGATTTAGAGCTTTAGAAGACCACAC-3′
35 Reverse	5′-GCTCTAAATCT**MNN**AGTTGGTGGATAGACAATCTTGGTTT-3′
113 Forward	5′-CAACCCAGTTG**NNK**TTTTTGGGAAGGGTTGCAGATCCAGC-3′
113 Reverse	5′-CTTCCCAAAAA**MNN**CAACTGGGTTGAAACGAAAGAACCG-3′
188 Forward	5′-ATATTGAACTC**NNK**GCTGCTCATGGCTACCTTTTAGATCA-3′
188 Reverse	5′-CCATGAGCAGC**MNN**GAGTTCAATATAGTCGAAACCAGCAT-3′
191 Forward	5′-TCCATGCTGCT**NNK**GGCTACCTTTTAGATCAATTTTTGCA-3′
191 Reverse	5′-AAAAGGTAGCC**MNN**AGCAGCATGGAGTTCAATATAGTCGA-3′

in both the $2mF_o$-F_c and F_o-F_c maps. Either malonate alone (3TJL) or nicotinamide (3UPW) completely accounted for this additional active site electron density. In the case of the *p*-chlorophenol soaked structure, the final electron density maps suggested only partial occupancy of this ligand (approximately 60%), consistent with the very short ligand soaking time. Additional electron density beyond that of *p*-chlorophenol was modeled as a malonate molecule in the same orientation as observed in the native structure. The deposited structure (4DF2) has both ligands in the model. All protein structure figures were created using PyMOL (Schrödinger, LLC).

Phenol Binding Studies

Assays were performed at 20 °C in 100 mM KP_i, pH 7.0 in a total volume of 1 mL. Purified OYE 2.6 was added to a final concentration of *ca.* 20 μM. The actual protein concentration present during each experiment was calculated from the initial value of A^{460} using $\varepsilon^{460} = 10{,}600$.[22a] Aliquots of the appropriate phenol (*p*-chlorophenol or *p*-hydroxybenzaldehyde; 4.0 mM stocks in EtOH) were added to the protein solution and the mixtures were stirred briefly. Spectra were recorded at *ca.* 1 min intervals until no further change was observed (typically $\leq$3 min). This process was continued until apparent saturation was reached.

Library Creation and Screening

Site saturation mutagenesis libraries were prepared by a modification of the methods reported by Zheng et al.[31] Each PCR mixture (total volume 100 μL) containing 5× Phusion HF Buffer (20 μL), template pBS2 (1 ng), forward and reverse NNK degenerate primers (0.5 μM each), dNTPs (200 μM each), and Phusion Hot Start II High-Fidelity DNA Polymerase (1 U) was subjected to an initial denaturation step of 98 °C (30 s) followed by 25 cycles of 98 °C (10 s) and 62–72 °C (4 min) followed by a final incubation at 72 °C (7 min). Primer sequences are shown in Table 2. Amplicons were purified by DNA spin columns, digested with *Dpn*I at 37 °C (10 U for 4 h followed by an additional 10 U for 4 h), then purified again by DNA spin columns. Aliquots (5 μL) were used to transform Electo-Ten Blue (Stratagene) electrocompetent cells (75 μL) by electroporation. SOC medium was added (600 μL), then samples were incubated for 1 h at 37 °C prior to selection on LB media plates supplemented with 200 $\mu g\,mL^{-1}$ ampicillin. After overnight incubation, all colonies from transformations yielding $\geq$ 300 c.f.u. from three combined plates were suspended in a small volume of LB medium, then pelleted by brief centrifugation. Pooled plasmid DNA was isolated by alkaline lysis, purified by spin columns and sequenced by automatic fluorescence methods to identify samples with the highest degree of degeneracy at the desired positions.

The pooled degenerate plasmid sample (1 ng) was used to transform 40 μL of electrocompetent BL21 Gold (DE3) cells. After recovery for 1 h at 37 °C in 600 μL of SOC medium, cells were spread on LB agar plates containing 200 $\mu g\,mL^{-1}$ ampicillin and incubated overnight at 37 °C. Ninety five individual transformants (plus a wild-type control) were used to seed a 2 mL deepwell plate and all 96 plasmids were prepared by rolling circle amplification and sequenced. Based on the sequencing data, clones representing each of the 32 possible codons (when available) were used to seed 600 μL of LB media containing 200 $\mu g\,mL^{-1}$ ampicillin arrayed on $^1/_3$ of a deepwell plate (2 mL total volume per well) to yield library master plates. The number of codons and amino acids obtained from each library are listed in Table 3.

When sequence data from the Ile 113 library were analyzed, OYE 2.6 genes encoding the Asp, Lys and Phe variants were missing. These were prepared individually by a modification of the method described above. For these amplifications, primers encoded only a single amino acid at position 113 (instead of NNK degeneracy), 20 ng of template (pBS2) were used and one extension temperature (72 °C) was employed; other conditions were identical. Amplicons were purified, digested with *Dpn*I and aliquots (5 μL) were used to transform *E. coli* JM109 cells (75 μL) by electroporation. Plasmid DNA was purified from randomly chosen colonies (spin columns) and sequenced to identify the missing OYE 2.6 variants. The appropriate plasmids were used to transform *E. coli* BL21 Gold (DE3) cells

Table 3. Library completeness data.

Position	Number of Sequences[a]	Unique codons	Unique amino acids
Thr 35	79	29	18
Ile 113	84	26	17[b]
His 188	92	31	19
His 191	91	28	16

[a] This indicates the subset of the 96 sequenced clones that provided usable data.

[b] The three missing amino acids were subsequently added to this library individually.

and the resulting strains were used to fill in the missing spaces in the Ile 113 library master plate.

Library screening plates were prepared from library master plates, either freshly grown in LB medium supplemented with 200 $\mu g\,mL^{-1}$ ampicillin or from frozen stocks. In the former case, the library master plate was shaken at 200 rpm and 37 °C. After 6 h, the cultures were visibly turbid and a 20-μL aliquot from each well was used to inoculate wells in a duplicate deepwell plate containing 600 μL of ZYP-5052 auto-inducing medium supplemented with 200 $\mu g\,mL^{-1}$ ampicillin. Alternatively, the auto-induction plates were inoculated directly from frozen library master plates. After seeding, library screening plates were then mounted in a growth apparatus designed to facilitate maximal oxygen transfer rates (based on the design of Duetz and Witholt[43]) and shaken at 300 rpm and 37 °C. After 16–18 h, cells were harvested by centrifuging at 3,000 rpm for 30 min and the supernatant was removed by aspiration. Cell pellets were resuspended in 300 μL of 50 mM KP_i, 100 mM glucose, 10 mM substrate, pH 7.0. The plate was shaken at 200 rpm at room temperature. After 6 h, wells were individually extracted with 500 μL of EtOAc prior to chiral-phase GC analysis.

Acknowledgements

Financial support by the National Science Foundation (CHE-0615776 and CHE-1111791) and the U.S. Army Advanced Civilian Schooling Program is gratefully acknowledged. We also thank Professor Steven Bruner for his generous guidance in crystallographic studies, Professor Robert McKenna and Dr. Arthur Robbins (U.F. Center for Structural Biology) for diffractometer access and many helpful discussions and Dr. Annie Héroux [Macromolecular Crystallography Research Resource (PXRR), National Synchotron Light Source] for crystallographic data collection.

References

[1] a) R. E. Williams, N. C. Bruce, *Microbiology* **2002**, *148*, 1607–1614; b) R. Stuermer, B. Hauer, M. Hall, K. Faber, *Curr. Opin. Chem. Biol.* **2007**, *11*, 203–213; c) H. S. Toogood, J. M. Gardiner, N. S. Scrutton, *ChemCatChem* **2010**, *2*, 892–914; d) M. Hall, A. S. Bommarius, *Chem. Rev.* **2011**, *111*, 4088–4110.

[2] Formerly known as *Saccharomyces carlsbergensis.*

[3] A. D. N. Vaz, S. Chakraborty, V. Massey, *Biochemistry* **1995**, *34*, 4246–4256.

[4] a) A. Z. Walton, W. C. Conerly, Y. Pompeu, B. Sullivan, J. D. Stewart, *ACS Catalysis* **2011**, *1*, 989–993; b) E. Brenna, F. G. Gatti, A. Manfredi, D. Monti, F. Parmeggiani, *Eur. J. Org. Chem.* **2011**, 4015–4022.

[5] P. F. Mugford, U. G. Wagner, Y. Jiang, K. Faber, R. J. Kazlauskas, *Angew. Chem.* **2008**, *120*, 8912–8923; *Angew. Chem. Int. Ed.* **2008**, *47*, 8782–8793.

[6] D. J. Bougioukou, *Ph.D. thesis*, University of Florida (Gainesville, FL, USA), **2006**.

[7] S. K. Padhi, D. J. Bougioukou, J. D. Stewart, *J. Am. Chem. Soc.* **2009**, *131*, 3271–3280.

[8] a) Also known as *Scheffersomyces stipitis*; b) T. W. Jeffries, I. V. Grigoriev, J. Grimwood, J. M. Laplaza, A. Aerts, A. Salamov, J. Schmutz, E. Lindquist, P. Dehal, H. Shapiro, Y.-S. Jin, V. Passoth, P. M. Richardson, *Nature Biotech.* **2007**, *25*, 319–326.

[9] D. J. Bougioukou, A. Z. Walton, J. D. Stewart, *Chem. Commun.* **2010**, *46*, 8558–8560.

[10] A. S. Abramovitz, V. Massey, *J. Biol. Chem.* **1976**, *251*, 5321–5326.

[11] B. W. Matthews, *J. Mol. Biol.* **1968**, *33*, 491–497.

[12] P. D. Adams, P. V. Afonine, G. Bunkoczi, V. B. Chen, I. W. Davis, N. Echols, J. J. Headd, L. W. Hung, G. J. Kapral, R. W. Grosse-Kunstleve, A. J. McCoy, N. W. Moriarty, R. Oeffner, R. J. Read, D. C. Richardson, J. S. Richardson, T. C. Terwilliger, P. H. Zwart, *Acta Crystallogr. Sect. D* **2010**, *66*, 213–221.

[13] K. M. Fox, P. A. Karplus, *Structure* **1994**, *2*, 1089–1105.

[14] N. Nagano, C. A. Orengo, J. M. Thornton, *J. Mol. Biol.* **2002**, *321*, 741–765.

[15] T. Barna, H. L. Messiha, C. Petosa, N. C. Bruce, N. S. Scrutton, P. C. F. Moody, *J. Biol. Chem.* **2002**, *277*, 30976–30983.

[16] T. M. Barna, H. Khan, N. C. Bruce, I. Barsukov, N. S. Scrutton, P. C. F. Moody, *J. Mol. Biol.* **2001**, *310*, 433–447.

[17] K. Kitzing, T. B. Fitzpatrick, C. Wilken, J. Sawa, G. P. Bourenkov, P. Macheroux, T. Clausen, *J. Biol. Chem.* **2005**, *280*, 27904–27913.

[18] V. B. Chen, W. B. Arendall, J. J. Headd, D. A. Keedy, R. M. Immormino, G. J. Kapral, L. W. Murray, J. S. Richardson, D. C. Richardson, *Acta Crystallogr. Sect. D* **2010**, *66*, 12–21.

[19] K. Saito, D. J. Thiele, M. Davio, O. Lockridge, V. Massey, *J. Biol. Chem.* **1991**, *266*, 20720–20724.

[20] E. Krissinel, K. Henrick, *J. Mol. Biol.* **2007**, *372*, 774–797.

[21] a) D. Xu, R. M. Kohli, V. Massey, *Proc. Natl. Acad. Sci. USA* **1999**, *96*, 3556–3561; b) B. J. Brown, J. W. Hyun, S. Duvvuri, P. A. Karplus, V. Massey, *J. Biol. Chem.* **2002**, *277*, 2138–2145.

[22] a) R. G. Matthews, V. Massey, *J. Biol. Chem.* **1969**, *244*, 1779–1786; b) R. G. Matthews, V. Massey, C. C. Sweeley, *J. Biol. Chem.* **1975**, *250*, 9294–9298; c) A. S. Abramovitz, V. Massey, *J. Biol. Chem.* **1976**, *251*, 5327–5336.

[23] B. J. Brown, Z. Deng, P. A. Karplus, V. Massey, *J. Biol. Chem.* **1998**, *273*, 32753–32762.

[24] R. C. Stewart, V. Massey, *J. Biol. Chem.* **1985**, *260*, 3639–3647.

[25] While this electron density could also be fit well by benzoate, we favor nicotinamide since it was present in the bacterial growth medium while benzoate was not.

[26] M. W. Fraaije, A. Mattevi, *Trends Biochem. Sci.* **2000**, *25*, 126–132.

[27] B. V. Adalbjörnsson, H. Toogood, A. Fryszkowska, C. R. Pudney, T. A. Jowitt, D. Leys, N. S. Scrutton, *ChemBioChem* **2010**, *11*, 197–207.

[28] C. R. Pudney, S. Hay, J. Y. Pang, C. Costello, D. Leys, M. J. Sutcliffe, N. S. Scrutton, *J. Am. Chem. Soc.* **2007**, *129*, 13949–13956.

[29] a) C. Stueckler, C. K. Winkler, M. Bonnekessel, K. Faber, *Adv. Synth. Catal.* **2010**, *352*, 2663–2666; b) A. Chen, J. Xu, W. Chiang, C. L. L. Chai, *Tetrahedron*

2010, *66*, 1489–1495; c) N. Mase, A. Inoue, M. Nishio, K. Takabe, *Bioorg. Med. Chem. Lett.* **2009**, *19*, 3955–3958.
[30] a) C. Pautigny, S. Jeulin, T. Ayad, A. Zhang, J.-P. Genêt, V. Ratovelomanana-Vidal, *Adv. Synth. Catal.* **2008**, *350*, 2525–2532; b) J. Wassenaar, M. Kuil, M. Lutz, A. L. Spek, J. N. H. Reek, *Chem. Eur. J.* **2010**, *16*, 6509–6517; c) P. Etayo, J. L. Núñez-Rico, A. Vidal-Ferran, *Organometallics* **2011**, *30*, 6718–6725.
[31] L. Zheng, U. Baumann, J.-L. Reymond, *Nucl. Acids Res.* **2004**, *32*, e115.
[32] A. Yep, G. L. Kenyon, M. J. McLeish, *Proc. Natl. Acad. Sci. USA* **2008**, *105*, 5733–5738.
[33] M. Hulley, H. S. Toogood, A. Fryszkowska, D. Mansell, G. M. Stephens, J. M. Gardiner, N. S. Scrutton, *ChemBioChem* **2010**, *11*, 2433–2447.
[34] H. Toogood, A. Fryszkowska, M. Hulley, M. Sakuma, D. Mansell, G. M. Stephens, J. M. Gardiner, N. S. Scrutton, *ChemBioChem* **2011**, *12*, 738–749.
[35] A. Fryszkowska, H. Toogood, M. Sakuma, G. M. Stephens, J. M. Gardiner, N. S. Scrutton, *Catal. Sci. Technol.* **2011**, *1*, 948–957.
[36] D. J. Bougioukou, S. Kille, A. Taglieber, M. T. Reetz, *Adv. Synth. Catal.* **2009**, *351*, 3287–3305.
[37] C. Breithaupt, J. Straßner, U. Breitinger, R. Huber, P. Macheroux, A. Schaller, T. Clausen, *Structure* **2001**, *9*, 419–429.
[38] J. Sambrook, E. F. Fritsch, T. Maniatis, *Molecular Cloning. A Laboratory Manual*, 2nd edn., Cold Spring Harbor Press, Cold Spring Harbor, **1989**.
[39] F. W. Studier, *Protein Expression Purif.* **2005**, *41*, 207–234.
[40] S. Duvaud, M. R. Wilkins, R. D. Appel, A. Bairoch, in: *The Proteomics Handbook*, (Ed.: J. M. Walker), Humana Press, Totowa, NJ, **2005**, pp 571–607.
[41] Z. Otwinowski, W. Minor, *Meth. Enzymol.* **1997**, *276*, 307–326.
[42] P. Emsley, B. Lohkamp, W. G. Scott, K. Cowtan, *Acta Crystallogr. Sect. D* **2010**, *66*, 486–501.
[43] W. A. Duetz, B. Witholt, *Biochem. Eng. J.* **2001**, *7*, 113–115.

